Intention Prediction-Based Control for Vehicle Platoon to Handle Driver Cut-in

Yun Lu, *Member, IEEE*, Lingying Huang, Jiarong Yao, Rong Su, *Senior Member, IEEE*

***Abstract*—Vehicle platoons (VPs) are groups of vehicles driving together with a short inter-vehicle gap and a harmonized velocity. For a long period, the VPs and human-driven vehicles (HDVs) will coexist in mixed traffic flow, where the cut-in maneuver of the HDVs towards the VPs can be frequently expected. In this paper, to handle such cut-ins, we propose an intention prediction-based control method for the VPs by considering the tradeoff between the platoon integrity and traffic safety. Particularly, the proposed method is designed to prevent as many cut-ins as possible while taking care of the road safety. It consists of a cut-in prediction part, including intention and trajectory prediction algorithms, and a finite state machine (FSM)-based predictive control part, including a high-level FSM and a low-level predictive control. Driver-in-the-loop experiments were conducted in the VP-based driving scenarios to train the intention prediction algorithm and test the proposed method. We show the results detailing the control behavior of the proposed method in a no cut-in test, a mandatory cut-in test, and three discretionary cut-in tests. The results demonstrate that the proposed method can predict the cut-in intention of human drivers in real time. Besides, according to the prediction results, the proposed method can prevent cut-ins for the VPs while taking care of the road safety.**

***Index Terms*—Vehicle platoons, cut-in, intention prediction, predictive control.**

I. Introduction

VEHICLE platoons (VPs) are groups of vehicles driving together with a short inter-vehicle gap and a harmonized velocity, which are enabled by vehicle automation, as well as vehicle-to-vehicle or vehicle-to-infrastructure communications. Organizing multiple vehicles into a vehicle platoon (VP) is shown to be effective in increasing traffic throughput and mitigating traffic jam [1], [2]. Besides, the VPs have potential to improve the road safety and driving comfort [3], [4]. In addition, the vehicles of a platoon can decrease exhaust emissions and fuel consumption [5], [6]. Due to its advantages in intelligent transportation systems, the VP has attracted considerable attention in the academic and industry fields.

To obtain the expected benefits of the VPs, a major challenge is to deploy them in real traffic environment. The deployment of the VPs will be gradual due to the need of supporting road infrastructures [7], user acceptance [8], and suitable regulations and legislation frameworks [9]. It will take a long time to let them have dedicated areas or lanes. Before that, they have to share road with conventional human-driven vehicles (HDVs) in mixed traffic flow for a long period [10]. In this context, the HDVs can produce irregular driving behavior towards the VPs, which may influence the performance of the VPs [11]. Thus, it is necessary for the VPs to address the interactions with the HDVs.

Cut-in maneuver of the HDVs is an inter-vehicle interaction that can be frequently expected. In the cut-in scenarios, the lane-changing vehicle moves into the space ahead of a nearby following vehicle in the target lane. The following vehicle may adjust its following gap to respond to the cut-in via emergency acceleration or braking, which increases fuel consumption and affects traffic efficiency [12]. Furthermore, the cut-in maneuver is potentially dangerous and may lead to traffic collisions. In particular, such maneuver appears to be unavoidable in mixed traffic and is regarded as a common hazard for the VPs [11]. It can affect the integrity of the VPs, which makes platooning difficult.

For single vehicles, including the autonomous vehicles (AVs) and HDVs equipped with advanced driver assistance systems, great efforts have been made to handle the cut-in maneuver of the surrounding HDVs. Chen *et al.* [13] built a human-centered control method based on the driver behavior prediction for the AVs to follow the reference trajectory while cooperating with the cut-in vehicle. In [14], a human-like car-following (CF) model was built for the AVs by considering the cut-in behavior of other vehicles in mixed traffic. Chen *et al.* [15] established an intelligent speed control strategy and a reinforcement learning method for the AVs to handle uncertain cut-in scenarios. In [16], a behavior estimation method was built to recognize and predict the cut-in intention for the CF control in the autonomous driving. Choi *et al.* [17] designed a cut-in warning system by using multiple rotational images of surround view monitoring cameras. Lyu *et al.* [18] developed a cut-in collision warning model to improve the effectiveness of advanced driver assistance systems in cut-in scenarios.

For the VPs, however, the methods built for single vehicles to address the cut-ins may not be suitable, due to the difference between the control objectives of the VPs and single vehicles. Different from a single vehicle, the VP has the control objective of maintaining the platoon integrity, which conflicts with the cut-in objective of the HDVs. Recently, a few studies have been carried out for the VPs to handle the cut-ins. Milanés *et al.* [19]

Manuscript received June 13, 2022, revised October 1, 2022, December 1, 2022, and January 17, 2023, accepted January 22, 2023. This work was supported by A*STAR under its RIE2020 Advanced Manufacturing and Engineering (AME) Industry Alignment Fund C Pre-Positioning (IAF-PP) (LOA Award A19D6a0053). *(Corresponding author: Rong Su)*

The authors are with the School of Electrical and Electronic Engineering, Nanyang Technological University, Singapore 639798 (e-mail: yun.lu@ntu.edu.sg; lingying.huang@ntu.edu.sg; jiarong.yao@ntu.edu.sg; rsu@ntu.edu.sg).

designed an algorithm for the VP to manage the transitions in response to the cut-ins from other vehicles. They tested the algorithm by using a string of four cooperative adaptive cruise control vehicles in real traffic condition. In [20], a control method was developed for the VPs to decrease the effect of vehicle cut-ins. Kazemi *et al.* [21] established a cooperative adaptive cruise control system by using a learning-based stochastic model predictive control (MPC), which can address the cut-in maneuvers of the HDVs. In [22], an MPC method was built to control a dynamic VP while handling possible cut-in/out maneuvers. Yao *et al.* [23] developed a decentralized lane-change-aware trajectory optimization model for trajectory smoothing of the connected automated vehicles at a signalized intersection. The model integrated the strategies of yielding to mandatory lane change and restraining discretionary lane change. Liu *et al.* [24] built a sensor fusion algorithm based on the radar and vision data for the VPs to recognize the cut-in vehicles.

When handling the cut-ins of the HDVs, the control method for the VPs faces a tradeoff between the platoon integrity and road safety. On the one side, preventing the cut-ins is beneficial to the integrity and performance of the VPs, but may result in vehicle accident and traffic congestion. On the other side, yielding to the cut-ins could improve driving safety and the overall traffic flow, but may break up the VP and lower its fuel efficiency [10]. To achieve the benefits of the VPs and take care of the traffic safety at the same time, it is important to consider such tradeoff in the controller design of the VPs. However, to the best of our knowledge, no study has designed control scheme for the VPs to address the cut-ins by considering such tradeoff.

Furthermore, the existing control methods built for the VPs to address the cut-ins do not incorporate the prediction of the driver intention. The significance of integrating such prediction in the control method is twofold: 1) it can help the VP better assess the potential cut-ins, and thus improve the road safety; 2) it enables the VP to respond to the cut-ins as early as possible, and thus to be more active when facing the cut-ins.

Thus, to address the cut-ins of the HDVs, this paper proposes a novel method for the VPs by incorporating the prediction of the driver intention and considering the tradeoff between the platoon integrity and road safety. In particular, the proposed method is developed to prevent as many cut-ins as possible while taking care of the road safety. It consists of a cut-in prediction part and a finite state machine (FSM)-based predictive control part. In the cut-in prediction part, a new support vector machine (SVM)-based algorithm is designed to predict the cut-in intention of human drivers; a trajectory prediction algorithm is used to predict the trajectory of the HDV. In the FSM-based predictive control part, a novel FSM and novel MPC algorithms are built to implement the control objectives of the proposed method. The main contributions of this study are as follows: 1) it addresses the cut-ins for the VP by considering the tradeoff between the platoon integrity and road safety; 2) it handles the cut-ins for the VP by incorporating the prediction of the driver intention; 3) it designs a novel SVM-based algorithm to predict driver cut-in intention towards a platoon; 4) it designs a novel control method based on the FSM and MPC to prevent as many cut-ins as possible for the platoon while taking care of the road safety; 5) it verifies the effectiveness of the proposed scheme with driver-in-the-loop experiments in the VP-based driving scenarios.

The remainder of this paper is organized as follows. Section II presents the architecture of the proposed method. Sections III and IV introduce the cut-in prediction part and the FSM-based predictive control part, respectively. Section V describes the driver-in-the-loop experiments for testing the proposed method, whose results are presented in Section VI. Finally, Section VII provides the discussion and conclusion of this paper.

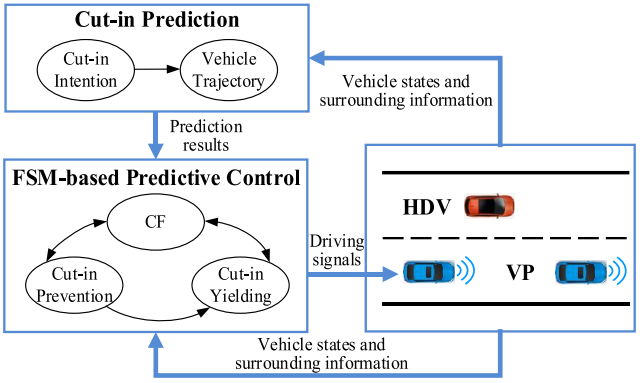

Fig. 1. Structure of the intention prediction-based control method.

II. System Architecture

The intention prediction-based control method is proposed for the VPs to handle the cut-in maneuvers of the HDVs. Note that how often a VP encounters the cut-ins should depend on the traffic condition, e.g., traffic flow. As shown in Fig. 1, the proposed method consists of two parts: 1) cut-in prediction, which predicts the cut-in intention of human drivers and the trajectory of the HDV; 2) FSM-based predictive control, which implements the control objective of the proposed method with three control strategies, i.e., CF, cut-in prevention, and cut-in yielding strategies. The working procedure of the proposed method is as follows. The cut-in prediction part first predicts the cut-in intention of the nearby HDVs according to the states of the HDVs and the relative states between the VP and HDVs. Then, the prediction part predicts the trajectories of the HDVs in a prediction horizon. Next, according to the predicted results, the VP states, and the surroundings, the FSM-based predictive control part employs the FSM to choose a control strategy from the CF, cut-in prevention, and cut-in yielding strategies. Finally, to implement the selected control strategy, the control part conducts the longitudinal control of the VP by using an MPC controller.

A. Cut-in Prediction

The cut-in prediction part is built for the proposed method to better assess the potential cut-ins and respond to the cut-ins as early as possible. This part includes two algorithms: cut-in intention and vehicle trajectory prediction algorithms. In the intention prediction algorithm, the cut-in intention of the

nearby HDVs is predicted by using the SVM, which is a supervised learning method that has been widely employed to predict driver intention [25], [26]. Particularly, the algorithm is built to predict whether the nearby HDVs intend to perform cut-in towards the platoon. The vehicle trajectory prediction algorithm predicts the trajectory of the HDV in a prediction time step. The trajectory is characterized by the lateral and longitudinal displacements of the vehicle, which are calculated by using a preview model and a longitudinal dynamic model, respectively. The predicted results are used in the FSM-based predictive control part for selecting a control strategy from the CF, cut-in prevention, and cut-in yielding strategies.

B. FSM-Based Predictive Control

The FSM-based predictive control part is built to implement the control objective of the proposed method, which is to prevent as many cut-ins as possible for the VP while taking care of the road safety. This part is divided into two levels: a high-level FSM and a low-level predictive control. The FSM decides the control strategy used in the low-level predictive control. The FSM has three states, i.e., CF, cut-in prevention, and cut-in yielding states, which correspond to the three control strategies of the VP, respectively. The transitions between these states are managed by using the predicted cut-in intention, the predicted vehicle trajectory with respect to the VP, and the surrounding information. The low-level predictive control has three control strategies: the CF, cut-in prevention, and cut-in yielding strategies. They are implemented via the MPC method as it can integrate multiple objectives into an optimization problem and adapt to the disturbances and uncertainties with a receding horizon strategy [27], [28]. In the CF strategy, the driving objective of the VP is to maintain a defined distance from the preceding vehicle while ensuring the ride comfort. In the cut-in prevention strategy, the control objective of the VP is to shorten the platoon gap while maintaining the ride comfort and driving safety. In the cut-in yielding strategy, the control objective of the VP is to create a safe distance from the cut-in vehicle while keeping the ride comfort.

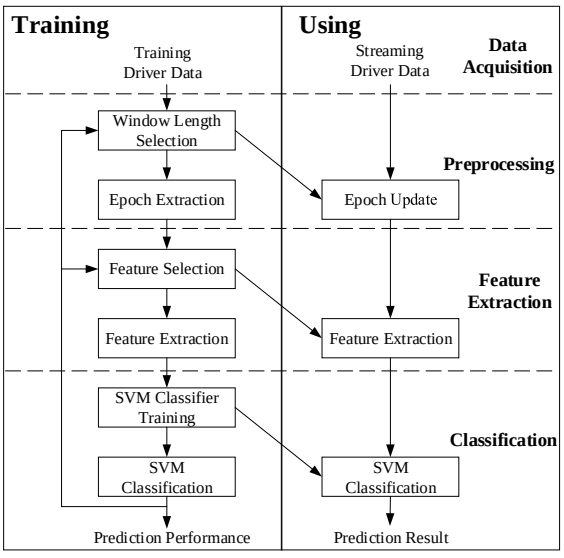

Fig. 2. Algorithm flow of the cut-in intention prediction.

III. CUT-IN PREDICTION

In Section III-A, we present the details of using an algorithm to predict the cut-in intention of the nearby HDV. In Section III-B, we describe how to apply a lateral preview model and a longitudinal dynamic model to predict the trajectory of the HDV.

A. Cut-in Intention Prediction

The aim of the intention prediction is to know whether the nearby HDVs intend to conduct cut-in towards the VP. Thus, the intention prediction problem can be regarded as a binary classification problem. As shown in Fig. 2, the algorithm of the intention prediction consists of training and using procedures. The offline training procedure is employed to calculate the parameters and the prediction performance of the algorithm. The online using procedure is applied to decode the streaming driving data into the prediction result in real time. The two procedures include four parts: data acquisition, preprocessing, feature extraction, and classification.

1) Data Acquisition

Driver-in-the-loop experiment is conducted to collect driver data in the mixed traffic flow, which includes the VP and HDV. The collected driving data include the lateral, longitudinal, and yaw data. The experimental platform is built by using a driving simulator, simulated vehicles, and a virtual scene. In the experiment, the drivers are asked to perform cut-in towards the VP and lane-retention to obtain two classes of training samples. The training driver data are recorded with labels of the cut-in intention, whereas the streaming driver data are collected without knowing their corresponding intentions a priori.

Remark 1: In real world, the driving data are collected with automotive sensing, which can be divided into self-sensing, localization, and surrounding-sensing [29]. Self-sensing uses proprioceptive sensors, such as odometers and gyroscopes, to measure the states of the ego car. Localization, using external sensors such as GPS, determines the global and local position of the ego car. Surrounding-sensing uses exteroceptive sensors, such as sonar, radar, and cameras, to perceive road information and the states of other vehicles. The VP can detect the states of the HDV by using exteroceptive sensors in real world.

2) Preprocessing

In the decoding process, epochs of the driving data with certain time window length are extracted as single units to be translated into the prediction results. In the training procedure, the epochs are extracted from the instant when the cut-in intention is labelled. We try different time window lengths and select one for use. In the using procedure, we adopt the selected time window length and update the epochs by using the historical driving data of the current time step.

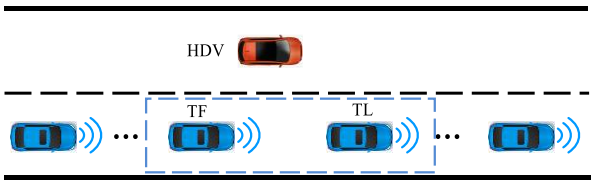

Fig. 3. Target vehicles related to the cut-in task.

3) Feature Extraction

We extract the features of the epochs to distinguish different classes of driving data. The selected features consist of the features related to the states of the nearby HDV and the relative states between the HDV and VP. Note that, in the VP, we only focus on the target leader (TL) and target follower (TF) related to the cut-in task. As shown in Fig. 3, the TL and TF refer to the front and rear vehicles of the target gap, respectively. The features related to the states of the HDV include its yaw angles, lateral and longitudinal velocities, and lateral and longitudinal accelerations at the initial and final instants of the epoch, along with their increments in the selected time window length. The features associated with the relative states between the HDV and VP consist of the relative velocities and longitudinal distances between the HDV and TF and the time headway and inverse time-to-collision between the HDV and TL at the initial and final instants of the epoch, and their increments in the selected time window length. The time headway and inverse time-to-collision are defined as

$$THW = \frac{D_{hl}}{v_h} \tag{1}$$

$$TTCi = \frac{v_{hl}}{D_{hl}} \tag{2}$$

where v_h is the longitudinal velocity of the HDV, D_{hl} is the relative distance between the HDV and TL, and v_{hl} is the relative velocity between the two vehicles.

4) Classification

A binary classifier is built to handle the binary classification problem. Particularly, we build the classifier by using the SVM with a radial basis function as the kernel function. The classifier is described as

$$y = \sum_{i=1}^{M} w_i \exp(-g \left\| x_i - x \right\|^2) + b \tag{3}$$

where M denotes the number of the support vector, w_i is the weight of the ith support vector, x_i is the ith support vector, x is a vector of the extracted features, including the time headway and inverse time-to-collision computed in (1) and (2), and b is the bias of the classifier. In the training procedure, the LIBSVM software library developed by Chang and Lin [30] is used to determine the parameters of the classifier.

Remark 2: We use the SVM to develop the binary classifier due to the following reasons. The SVM has the advantage of producing more robust models than traditional learning methods by minimizing the upper bound of the generalization error [31]. Besides, the SVM can extract pattern from noisy data without prior knowledge before training [32].

B. Vehicle Trajectory Prediction

The trajectory of the HDV is predicted so that the proposed method can know its driving tendency and then accordingly decide the control strategy of the VP. The prediction of the vehicle trajectory is separated into the predictions of the lateral and longitudinal displacements of the vehicle.

We apply the method described in [13] to predict the lateral position of the vehicle. The lateral position is predicted based on the driver preview behavior of previewing the future desired path in a preview interval. The preview point of the driver model can be calculated as

$$y_p = y_0 + v_h \tau e_\psi \tag{4}$$

where y_0 is the current lateral position of the vehicle, y_p is the lateral position of the vehicle at the preview point, τ denotes the preview time, and e_ψ represents the yaw angle error, which is computed as

$$e_\psi = \psi_h - \psi_d \tag{5}$$

where ψ_h is the yaw angle of the vehicle and ψ_d is the desired yaw angle.

Based on the equation (4), the prediction model of the lateral vehicle position can be described as

$$y_h^{(k+1)} = y_h^{(k)} + T v_h^{(0)} e_\psi^{(0)}, \ k = 0, \cdots, N_p - 1 \tag{6}$$

where $y_h^{(k)}$ is predicted lateral position of the vehicle at time step k, $y_h^{(0)}$, $v_h^{(0)}$, and $e_\psi^{(0)}$ are the measured values at the current time step, T is the sampling time, and N_p is preview horizon.

Remark 3: Note that the drivers may first prepare to cut-in and then execute cut-in after generating the cut-in intention [33]. They desire to drive in the original and target lanes in the cut-in preparation and execution phases, respectively. In other words, the preview point is on the centerline of the original and target lanes in the two phases, respectively. In the same spirit of [18], we set the threshold value of the lane-change offset rate as 0.15 m/s to represent the beginning of the cut-in execution phase.

Assuming the HDV drives with the longitudinal acceleration of the current time step in the prediction horizon, we formulate the prediction model of the longitudinal vehicle position as

$$s_h^{(k+1)} = s_h^{(k)} + T v_h^{(0)} + \frac{T^2}{2} a_h^{(0)}, \ k = 0, \cdots, N_p - 1 \tag{7}$$

where $s_h^{(k)}$ is the predicted longitudinal displacement of the vehicle at time step k and $a_h^{(0)}$ is its longitudinal acceleration at the current time step.

Remark 4: The lateral speed and longitudinal acceleration are assumed to be constant in a prediction horizon. The assumption (also used in [13] and [34]) is considered reasonable because the prediction horizon is a few seconds ahead and the speed and acceleration update at each time step, which decrease the influence of the assumption errors.

IV. FSM-BASED PREDICTIVE CONTROL

The overall objective of the FSM-based predictive control is to prevent as many cut-ins as possible for the VP while taking care of the road safety. In Section IV-A, we explain how to build the high-level FSM. In Section IV-B, we describe the algorithms of the low-level predictive control.

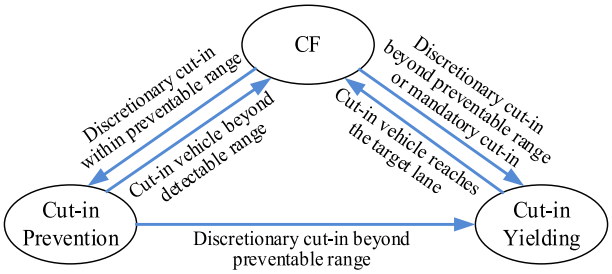

Fig. 4. Architecture of the high-level FSM.

A. High-Level FSM

The high-level FSM is built to select control strategy for the VP to handle the cut-ins. As shown in Fig. 4, the FSM consists of three states: the CF, cut-in prevention, and cut-in yielding states. In the CF state, the followers of the VP perform CF to maintain a defined distance from the preceding vehicle. In the cut-in prevention state, the VP shortens the platoon gap to prevent the cut-ins of the HDV. In the cut-in yielding state, the VP yields to the cut-in vehicle by creating a safe distance.

The state transitions are managed according to the predicted cut-in intention, the surrounding information, and the predicted trajectory of the HDV with respect to the VP. The predicted cut-in intention indicates whether the nearby HDV intends to conduct cut-in towards the VP. According to the surrounding information, we classify the cut-in motivation into the mandatory and discretionary cut-ins. The mandatory cut-ins refer to the situation where drivers must perform cut-ins to leave the current lane, e.g., to use an on-ramp to enter a freeway or to avoid obstacles [35]. The discretionary cut-ins refer to the situation where drivers conduct cut-ins to move into a target lane with a more desirable driving condition. The predicted vehicle trajectory is used to calculate whether the HDV is in the defined preventable range. When the vehicle was predicted to drive across the lane marks and have a vehicle-length lead over the TF, it was considered in the unpreventable range. Otherwise, it was considered in the preventable range. Note that the HDV predicted to drive in the unpreventable range is regarded as a cut-in vehicle.

In the CF state, the FSM can be switched to the cut-in prevention and yielding states. If the nearby HDV is predicted to have no cut-in intention, the FSM remains in the CF state. If it is predicted to have the discretionary cut-in intention and the cut-in vehicle is predicted to drive in the preventable range, the FSM is switched to the cut-in prevention state. If the HDV suggests the mandatory cut-in intention, the FSM is switched to the cut-in yielding state. If it indicates the discretionary cut-in intention and is predicted to drive in the unpreventable range, the FSM is switched to the cut-in yielding state.

In the cut-in prevention state, the FSM can be switched to the CF and cut-in yielding states. If the cut-in vehicle remains in the preventable and detectable range, the FSM remains in the cut-in prevention state. If the cut-in vehicle does not perform cut-in and is out of the detectable range, the FSM is switched to the CF state. If the cut-in vehicle is predicted to drive in the unpreventable range, the FSM is switched to the cut-in yielding state.

In the cut-in yielding state, if the cut-in vehicle reaches the target lane, the FSM is switched to the CF state. Otherwise, the FSM remains in the cut-in yielding state.

B. Low-Level Predictive Control

The low-level predictive control is developed to implement the control strategy decided in the high-level FSM. Particularly, three MPC algorithms are formulated based on the control strategies of the CF, cut-in prevention, and cut-in yielding, respectively. In the algorithms, the vehicle longitudinal models are applied as the prediction models.

1) Vehicle Longitudinal Model

In the VP, the TF is controlled to address the cut-ins of the HDVs. The controlled vehicle, i.e., the TF, is expected to imperfectly track its desired acceleration. We describe its dynamic model with a first-order lag as

$$\tau \dot{a} + a = u \tag{8}$$

where u and a represent the desired and actual longitudinal accelerations of the controlled vehicle, respectively, and τ is the time lag [36].

Integrating forward difference approximations, the model in (8) can be rewritten as

$$x^{(k+1)} = Ax^{(k)} + Bu^{(k)},$$
$$A = \begin{bmatrix} 1 & T & 0 \\ 0 & 1 & T \\ 0 & 0 & 1-T/\tau \end{bmatrix}, \ B = \begin{bmatrix} 0 \\ 0 \\ T/\tau \end{bmatrix}. \tag{9}$$

where $x^{(k)} = [s^{(k)}, v^{(k)}, a^{(k)}]^T$ is the state variable of the controlled vehicle at time step k. s and v are the absolute position and longitudinal velocity of the controlled vehicle, respectively.

The preceding vehicle of the controlled vehicle can be either the TL or cut-in vehicle. We assume the preceding vehicle has a constant acceleration in the prediction horizon. Its longitudinal model can be expressed as

$$x_i^{(k+1)} = A_T x_i^{(k)}, \ i \in \{c, l\}$$
$$A_T = \begin{bmatrix} 1 & T & T^2/2 \\ 0 & 1 & T \\ 0 & 0 & 1 \end{bmatrix}. \tag{10}$$

where $x_c = [s_c, v_c, a_c]^T$ and $x_l = [s_l, v_l, a_l]^T$ are the state variables of the cut-in vehicle and TL, respectively. s_c and s_l are the absolute positions; v_c and v_l denote the longitudinal velocities; a_c and a_l represent the longitudinal accelerations.

2) Predictive Control for CF

To implement the CF strategy, the MPC algorithm is designed to include a CF and a smooth control objective. We add penalties on the longitudinal acceleration and its increment in the cost function to realize the smooth control objective. The CF objective is achieved by introducing penalties on the deviation from a desired inter-vehicle gap and the relative velocity between the controlled vehicle and its preceding vehicle in the cost function. The penalties are formulated as

$$J_1 = \sum_{k=0}^{N_1-1} (\alpha_1^{(k)} (S^{(k)} - S_d^{(k)})^2 + \beta_1^{(k)} (v_r^{(k)})^2) \tag{11}$$

where $S^{(k)}$ and $S_d^{(k)}$ are the inter-vehicle distance and desired distance at time step *k*, respectively, $v_r^{(k)}$ is the relative velocity between the control vehicle and its preceding vehicle, $\alpha_1^{(k)}$ and $\beta_1^{(k)}$ are the weights penalizing the distance deviation and relative velocity, respectively, and N_1 denotes the control horizon as well as the prediction horizon of the MPC algorithm. We compute the inter-vehicle distance, relative velocity, and desired distance as

$$S^{(k)} = s_i^{(k)} - s^{(k)} \tag{12}$$

$$v_r^{(k)} = v_i^{(k)} - v^{(k)} \tag{13}$$

$$S_d^{(k)} = v_i^{(k)} t_d + D_s, \; i = c \text{ or } l \tag{14}$$

where t_d is the desired time gap and D_s represents the desired standstill distance, which are set according to the defined platoon gap. In (12)–(14), *i* equals to *c* and *l* when the preceding vehicle of the TF is the cut-in vehicle and TL, respectively.

Remark 5: There are two major spacing policies for platoons: constant time-gap policy and constant distance policy. This study uses constant time-gap policy because it can ensure string stability by just using on-board information [37], [38] and it accords with driver behaviors to some extent [39].

Based on the above descriptions, the control algorithm for CF is formulated as

$$\min_{u} \sum_{k=0}^{N_1-1} (\alpha_1^{(k)} (S^{(k)} - S_d^{(k)})^2 + \beta_1^{(k)} (v_r^{(k)})^2 + \gamma_1^{(k)} (u^{(k)})^2 + \theta_1^{(k)} (\Delta u^{(k)})^2) \tag{15a}$$

$$\text{s.t.} \quad x^{(k+1)} = Ax^{(k)} + Bu^{(k)} \tag{15b}$$

$$x_i^{(k+1)} = A_T x_i^{(k)} \qquad i = c \text{ or } l \tag{15c}$$

$$\Delta u^{(k)} = u^{(k)} - u^{(k-1)} \tag{15d}$$

$$u_{\min} \le u^{(k)} \le u_{\max} \qquad k = 0, \cdots, N_1 - 1 \tag{15e}$$

$$x^{(0)} = x_0 \tag{15f}$$

$$x_c^{(0)} = x_{c0} \tag{15g}$$

$$x_l^{(0)} = x_{l0} \tag{15h}$$

where $\gamma_1^{(k)}$ and $\theta_1^{(k)}$ are the weights penalizing the longitudinal acceleration and its increment at time step *k*, respectively, and x_0, x_{c0}, and x_{l0} represent the current states of the controlled vehicle, cut-in vehicle, and TL, respectively. The equations (15b) and (15c) are the longitudinal models of the controlled vehicle and its preceding vehicle, respectively. The constraint (15d) is applied to compute the increment of the longitudinal acceleration. The constraint (15e) is the physical constraint. The constraints (15f)–(15h) ensure the states of the vehicles are initialized as the measured values of the current time step.

3) Predictive Control for Cut-in Prevention

To implement the cut-in prevention strategy, the control algorithm is built to shorten the platoon gap while maintaining the ride comfort and driving safety. We introduce penalties on the distance and relative velocity between the TL and TF to shorten the platoon gap. We add penalties on the longitudinal acceleration and its increment to maintain the longitudinal ride comfort. To keep the driving safety, we limit the distance between the TL and TF with a minimum speed-dependent distance strategy and a minimum time-to-collision strategy:

$$S_l^{(N_2)} \ge v^{(N_2)} t_{THD} + d_s \tag{16}$$

$$\frac{S_l^{(N_2)}}{v_{rl}^{(N_2)}} \ge t_{TTC} \tag{17}$$

where $S_l = s_l - s$ and $v_{rl} = v_l - v$ are the distance and relative velocity between the TL and TF, respectively, t_{THD} and t_{TTC} are the defined minimum time headway and time-to-collision, respectively, d_s is the minimum standstill distance, and N_2 denotes the prediction horizon of the control algorithm. Note that t_{THD} and d_s are set according to the defined safety distance. Integrating (16) and (17), we can derive

$$S_l^{(N_2)} \ge \max\{v^{(N_2)} t_{THD} + d_s, v_{rl}^{(N_2)} t_{TTC}\} \tag{18}$$

According to the above descriptions, we can formulate the optimization problem for cut-in prevention as

$$\min_{u,\varepsilon} \alpha_2 (S_l^{(N_2)})^2 + \beta_2 (v_{rl}^{(N_2)})^2 + \sum_{k=0}^{N_2-1} (\gamma_2^{(k)} (u^{(k)})^2 + \theta_2^{(k)} (\Delta u^{(k)})^2) + \rho_2 \varepsilon \tag{19a}$$

$$\text{s.t.} \quad x^{(k+1)} = Ax^{(k)} + Bu^{(k)} \tag{19b}$$

$$x_l^{(k+1)} = A_T x_l^{(k)} \tag{19c}$$

$$S_l^{(N_2)} \ge \max\{v^{(N_2)} t_{THD} + d_s, v_{rl}^{(N_2)} t_{TTC}\} - \varepsilon \tag{19d}$$

$$\Delta u^{(k)} = u^{(k)} - u^{(k-1)} \tag{19e}$$

$$u_{\min} \le u^{(k)} \le u_{\max} \qquad k = 0, \cdots, N_2 - 1 \tag{19f}$$

$$\varepsilon \ge 0 \tag{19g}$$

$$x^{(0)} = x_0 \tag{19h}$$

$$x_l^{(0)} = x_{l0} \tag{19i}$$

where α_2 and β_2 are the weights penalizing the distance and relative velocity between the TL and TF at time step N_2, respectively, $\gamma_2^{(k)}$ and $\theta_2^{(k)}$ are the weights penalizing the longitudinal acceleration and its increment at time step *k*, respectively, and ρ_2 is the weight penalizing the slack variable ε, which enables the constraint (19d) to be imposed as a soft constraint. In the cost function (19a), the first two terms are used to shorten the platoon gap; the third and fourth terms are applied to maintain the ride comfort. The constraint (19d) is derived by adding the slack variable into (18). The constraint (19g) limits the value range of the slack variable.

4) Predictive Control for Cut-in Yielding

To implement the cut-in yielding strategy, the MPC-based algorithm is designed to include a yielding objective, a smooth control objective, and a safety objective. The yielding objective is realized by adding penalties on the deviation from a desired inter-vehicle distance and the relative velocity between the TF and cut-in vehicle in the cost function. The smooth control

objective is achieved by adding penalties on the longitudinal acceleration and its increment in the cost function. To achieve the safety objective, we limit the distance between the TF and cut-in vehicle with the minimum speed-dependent distance strategy and the minimum time-to-collision strategy. We formulate the control algorithm for cut-in yielding as:

$$\min_{u,\varepsilon} \alpha_3 (S_c^{(N_3)} - S_d^{(N_3)})^2 + \beta_3 (v_{rc}^{(N_3)})^2 + \sum_{k=0}^{N_3-1} (\gamma_3^{(k)} (u^{(k)})^2 + \theta_3^{(k)} (\Delta u^{(k)})^2) + \rho_3 \varepsilon \quad (20a)$$

$$\text{s.t.} \quad x^{(k+1)} = Ax^{(k)} + Bu^{(k)} \quad (20b)$$

$$x_c^{(k+1)} = A_T x_c^{(k)} \quad (20c)$$

$$S_c^{(N_3)} \geq \max\{v^{(N_3)} t_{THD} + d_s, v_{rc}^{(N_3)} t_{TTC}\} - \varepsilon \quad (20d)$$

$$\Delta u^{(k)} = u^{(k)} - u^{(k-1)} \quad (20e)$$

$$u_{\min} \leq u^{(k)} \leq u_{\max} \qquad k = 0, \cdots, N_3 - 1 \quad (20f)$$

$$\varepsilon \geq 0 \quad (20g)$$

$$x^{(0)} = x_0 \quad (20h)$$

$$x_c^{(0)} = x_{l0} \quad (20i)$$

where $S_c = s_c - s$ and $v_{rc} = v_c - v$ are the distance and relative velocity between the TF and cut-in vehicle, respectively, N_3 is the prediction horizon, α_3 and β_3 are the weights penalizing the distance and relative velocity at time step N_3, respectively, $\gamma_3^{(k)}$ and $\theta_3^{(k)}$ are the weights penalizing the longitudinal acceleration and its increment at time step k, respectively, and ρ_3 denotes the weight penalizing the slack variable ε, which enables the constraint (20d) to be imposed as a soft constraint. In the cost function (20a), the first two terms are used to achieve the yielding objective; the third and fourth terms are applied to obtain the smooth control objective. The constraint (20d) is built for the safety objective.

The optimization problems including (15), (19), and (20) can be reformulated as the convex quadratic programming (CQP) problem, which is expressed as

$$\min_z \ q(z) = \frac{1}{2} z^T H z + z^T c \quad (21a)$$

$$\text{s.t.} \quad Ez \leq d \quad (21b)$$

where z is the optimization variable, H is a positive semidefinite matrix, c and d are real vectors, and E is a real matrix. The CQP problem is solved at each sampling instant with the latest measurements. Any local optimal solution of the CQP problem is the global one [40]. We only use the first signal of the optimal solution during the next sampling interval.

Remark 6: In the same spirit of [27] and [28], the safety constraints are set as soft constraints to guarantee safety as much as possible and avoid infeasibility of the optimization problem. Originally, the safety constraints are built as hard constraints, which could be violated because the safety cannot be guaranteed in arbitrary situations. To avoid infeasibility of the optimization problems, we change the hard constraints into the soft constraints by using the slack variables. Besides, we add penalties on the slack variables in the cost function and set the penalty weights as large values so that the algorithms are solved with the smallest possible slack variables for minimum loosening the constraints. In this way, the soft constraints can guarantee safety as much as possible.

Remark 7: The safety constraint is not included in the control algorithm for CF, but is included in the control algorithms for cut-in prevention and yielding. When the (potential) cut-ins are detected, the FSM will switch from the CF state to the cut-in prevention or yielding states. Thus, the fused algorithm can guarantee safety as much as possible for handling the cut-ins.

V. Driver-in-the-Loop Experiment

The driver-in-the-loop experiments were conducted under the VP-based driving scenarios to train the intention prediction algorithm and test the proposed method. We introduce the experimental setup and procedure in Sections V-A and B, respectively.

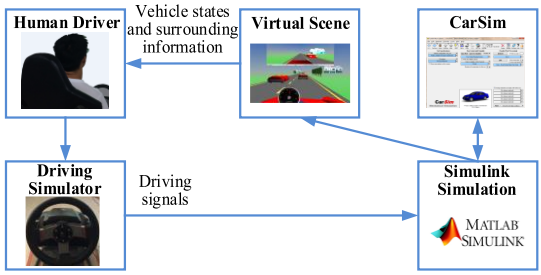

Fig. 5. Experimental platform.

TABLE I
Controller Parameters

Parameter	Symbol	Value	Unit
Weights penalizing distance	α_1, α_2, α_3	2	-
Weights penalizing relative velocity	β_1, β_2, β_3	2	-
Weights penalizing longitudinal acceleration	γ_1, γ_2, γ_3	1	-
Weights penalizing acceleration increment	θ_1, θ_2, θ_3	20	-
Weights penalizing slack variable	ρ_2, ρ_3	100	-
Prediction horizons	N_1, N_2, N_3	8	-
Sampling time	T	0.25	s
Desired time gap	t_d	0.6	s
Desired standstill distance	D_s	4.5	m
Maximum longitudinal acceleration	$u_{\max}$	2.5	m/s^2
Minimum longitudinal acceleration	$u_{\min}$	-2.5	m/s^2
Minimum time headway	t_{THD}	0.3	s
Minimum standstill distance	d_s	2	m
Minimum time-to-collision	t_{TTC}	1	s

A. Experimental Setup

As shown in Fig. 5, the experimental platform consisted of a driving simulator, simulated vehicles, and a virtual scene, which were connected by using Matlab/Simulink. The driving simulator from the Logitech Company provided pedals and a steering wheel for subjects to issue driving signals. The simulated vehicle controlled by users was implemented via the joint simulation of the Simulink and CarSim. The virtual scene

was written with virtual reality modeling language (VRML), which can help create interactive 3D scenes, and displayed via Simulink 3D Animation. In the virtual scene, we displayed the front and rear views of the HDV, along with its speedometer for presenting its velocity. Eight subjects (including five males and three females) aged 27–34 years voluntarily participated in the experiment without monetary compensation. They all had valid driver licenses for passenger cars. Their driving experience ranged from three to ten years with the average being 5.9 years. Fig. 6 shows the experimental scene. The parameters of the MPC controllers are listed in Table I.

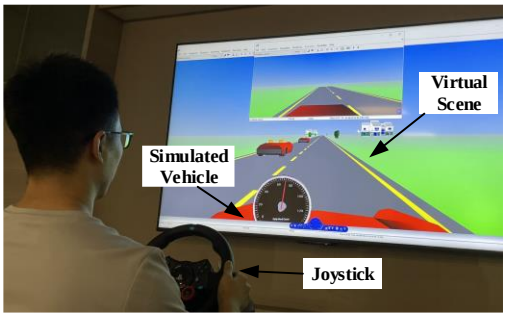

Fig. 6. Experimental scene.

Remark 8: The penalty weights in Table I are determined according to the priority of the penalties in the cost functions. The larger the penalty weight, the higher the priority of the corresponding penalty. In particular, the weights penalizing the slack variable are set to be the largest for encouraging the optimization problem to be solved without loosening the safety constraints; the weights penalizing the increment of the longitudinal acceleration are taken as the second largest to ensure that the smooth control objective has priority over other driving objectives.

B. Experimental Procedure

The experiment included two parts: 1) the participants were asked to perform some driving tasks to train the intention prediction algorithm; 2) driver-in-the-loop testing studies were conducted to test the proposed method. We explained the experimental purposes and procedures to the subjects before the start of the experiment. They were given about fifteen minutes of practice to get familiar with the driving simulator and virtual scene.

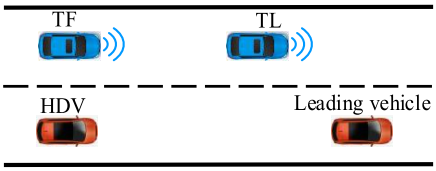

Fig. 7. Discretionary driving scenario.

In the training phase, a discretionary driving scenario was employed to collect driver data related to the lane-retention and cut-in maneuvers. We asked the subjects to drive the HDV to perform the lane-retention or cut-in maneuvers in the scenario. As shown in Fig. 7, the scenario was designed to include four vehicles on a two-lane (in the same direction) road. The four vehicles were made up of an HDV, a leading vehicle, and the TL and TF of a platoon. The leading vehicle was used to provide a reference for the HDV to perform the lane-retention maneuver. Its initial velocity was taken to be equal to the larger one of the HDV and target vehicles. Its initial position was set to be in front of the TL and HDV. The velocities of the leading vehicle and target vehicles were set to be constant in the driving process. We set two different initial velocities (i.e., 20 and 30 m/s) for the target vehicles. The initial velocity of the HDV was set to be -2, -1, 0, 1, and 2 m/s relative to the target vehicles. We selected ten different initial longitudinal positions for the HDV: one and two vehicle lengths away from, one and two vehicle lengths ahead of, and the same as one target vehicle (i.e., the TL or TF). We chose the time gaps of 0.8 and 0.6 s for the target vehicles driving at 20 and 30 m/s, respectively. We obtained 100 sub-scenarios by using different combination of the settings of the HDV and target vehicles.

Remark 9: Five times five-fold cross validation was used to evaluate the performance of the intention prediction algorithm. Table II shows the prediction accuracy of the algorithm under different time window lengths of the driving data. It refers to the accuracy of the algorithm in predicting whether the nearby vehicles intend to conduct cut-in towards the VP. Increasing the time window length improves the accuracy (as shown in Table II) but increases the response time of the algorithm at the same time. The time window length is chosen based on the tradeoff between the accuracy and response time. It was taken as 2 s in the testing phase.

TABLE II
PREDICTION ACCURACY OF THE INTENTION PREDICTION ALGORITHM

Time window length (s)	Accuracy (%)		
	Cut-in	Lane-retention	Mean
0.5	86.9	84.1	85.5
1.0	86.7	88.3	87.5
1.5	88.6	90.0	89.3
2.0	89.6	90.9	90.3
2.5	89.8	90.8	90.3
3.0	91.6	92.4	92.0
3.5	91.6	92.5	92.1
4.0	93.4	92.8	93.1

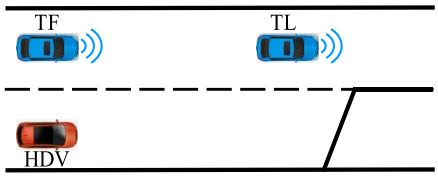

Fig. 8. Mandatory driving scenario.

In the testing phase, we employed the discretionary driving scenario and a mandatory driving scenario to test the proposed method. Fig. 8 presents the mandatory driving scenario. In the experiment, the subjects were given a cut-in or a lane-retention intention in the beginning and asked to control the HDV as they

would normally do in real-world driving environment. The TF was controlled by the proposed method to handle the cut-ins of the HDV. The testing results are described in Section VI.

VI. RESULTS

A. No Cut-in Test

We conducted the no cut-in test in the discretionary driving scenario, where the initial velocities of the HDV and target vehicles were 30 m/s and the initial longitudinal positons of the HDV and TF were the same. In this test, the driver controlled the HDV without the cut-in intention.

Remark 10: We show the FSM state of the proposed method to present the driving strategy of the TF. The state value is set equal to 2 and 3 when the TF works in the cut-in prevention and yielding strategies, respectively; it is set equal to 1 and 4 when the TF works in the CF strategy following the TL and cut-in vehicle, respectively. That is, when the state value equals to 4, the HDV has completed the cut-in towards the target vehicles.

The FSM state equals to 1 in the no cut-in test. That is, the TF works in the CF strategy following the TL all the time, which suggests the proposed method successfully infers the intention of the HDV. Figs. 9 (a) and (b) show the profiles of the longitudinal displacement and velocity of the vehicles in the no cut-in test, respectively. We see that, despite the HDV drives past the gap between the target vehicles, the TF drives at a constant velocity for maintaining a constant platoon gap.

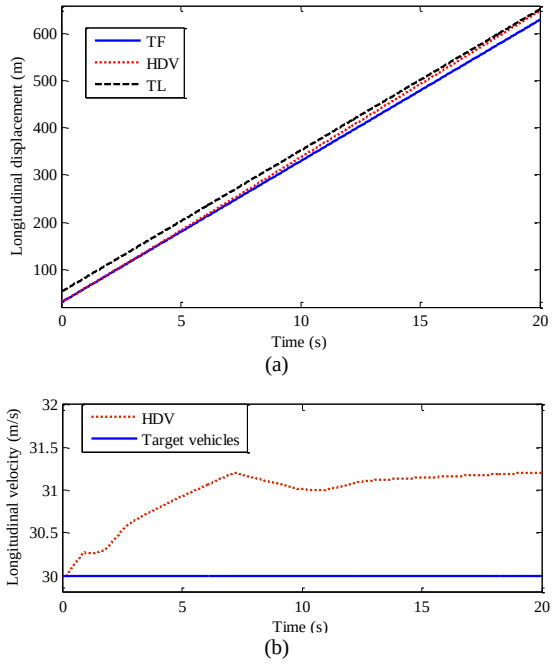

Figs. 9. Profiles of (a) longitudinal displacement and (b) velocity of the HDV and target vehicles in the no cut-in test.

B. Mandatory Cut-in Test

We conducted the mandatory cut-in test in the mandatory driving scenario, where the initial longitudinal positons of the HDV and TF were the same and the initial velocities of the three vehicles were 30 m/s. In the test, the driver controlled the HDV with the cut-in intention to avoid collision.

Fig. 10 presents the FSM state of the proposed method in the mandatory cut-in test. We see that the FSM state is switched from the CF state (following the TL) to the cut-in yielding state at 2.4 s, when the proposed method detects the cut-in intention of the HDV. Next, the FSM state is switched to the CF state (following the cut-in vehicle) at 5.4 s, when the cut-in vehicle reaches the target lane.

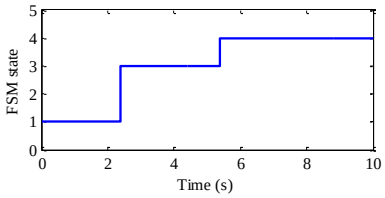

Fig. 10. FSM state of the proposed method in the mandatory cut-in test.

Figs. 11 (a), (b), and (c) show the profiles of the longitudinal displacement, lateral displacement, and longitudinal velocity of the HDV and target vehicles in the mandatory cut-in test, respectively. We see that the HDV speeds up to overtake the TF and then slows down to perform the cut-in and follow the TL. The TF keeps a constant velocity to follow the TL in the beginning, then slows down to yield to the HDV after detecting its cut-in intention, and finally speeds up to follow the cut-in vehicle.

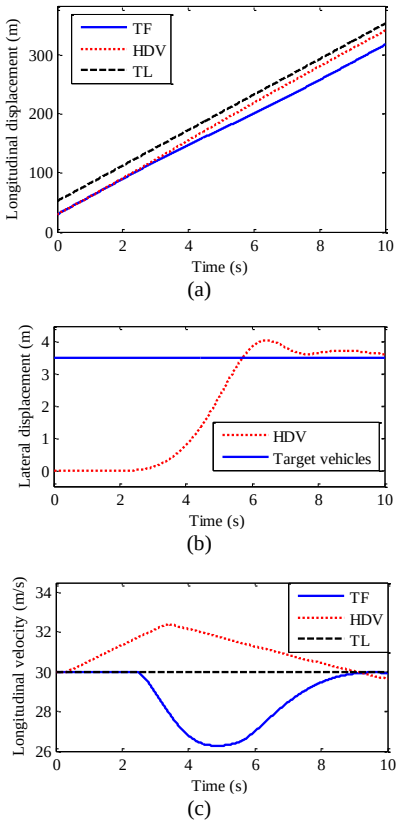

Figs. 11. Profiles of (a) longitudinal displacement, (b) lateral displacement, and (c) longitudinal velocity of the HDV and target vehicles in the mandatory cut-in test.

C. Discretionary Cut-in Test

We conducted the discretionary cut-in tests under three kinds of situations: cut-in within the preventable range, beyond the preventable range, and from within to beyond the preventable range. The tests were conducted in the discretionary driving scenario, where the initial velocities of the three vehicles were 30 m/s. In the scenario related to the discretionary cut-in within and from within to beyond the preventable range, the initial longitudinal positons of the HDV and TF were the same; in the scenario related to the cut-in beyond the preventable range, the initial longitudinal positon of the HDV was two vehicle lengths ahead of the TF.

1) Cut-in within Preventable Range

Fig. 12 presents the FSM state of the proposed method in handling the discretionary cut-in within the preventable range. We see the FSM state is switched from the CF state (following the TL) to the cut-in prevention state at 2.2 s, when the proposed method detects the cut-in intention of the HDV. The FSM state remains in the cut-in prevention state as the HDV is in the detectable range.

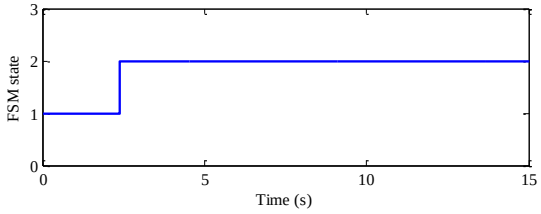

Fig. 12. FSM state of the proposed method in the discretionary cut-in (within the preventable range) test.

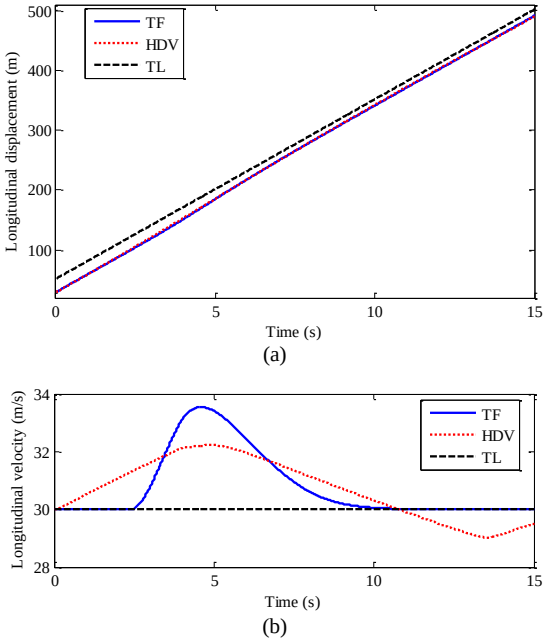

Figs. 13. Profiles of (a) longitudinal displacement and (b) velocity of the HDV and target vehicles in the discretionary cut-in (within the preventable range) test.

Figs. 13 (a) and (b) illustrate the profiles of the longitudinal displacement and velocity of the vehicles in the discretionary cut-in (within the preventable range) test, respectively. We see that the HDV speeds up to conduct the cut-in maneuver in the beginning and then slows down to give up the cut-in. The TF keeps a constant distance from the TL in the beginning, then shortens the platoon gap by accelerating and decelerating, and finally keeps the shortened gap with a constant velocity. In Fig. 13 (a), we see that there is no obvious difference between the longitudinal displacement of the HDV and TF. The reason for this is that the HDV drives beside the TF in the driving process.

2) Cut-in beyond Preventable Range

Fig. 14 illustrates the FSM state of the proposed method in handling the discretionary cut-in beyond the preventable range. We see the FSM state is switched from the CF state (following the TL) to the cut-in yielding state at 2.2 s, when the cut-in intention of the HDV is detected and the vehicle is beyond the preventable range. Then, the FSM state is switched to the CF state (following the cut-in vehicle) at 3.8 s, when the cut-in vehicle reaches the target lane.

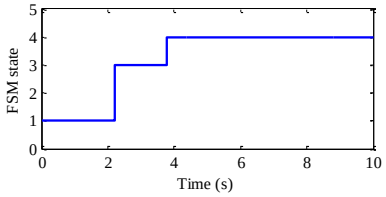

Fig. 14. FSM state of the proposed method in the discretionary cut-in (beyond the preventable range) test.

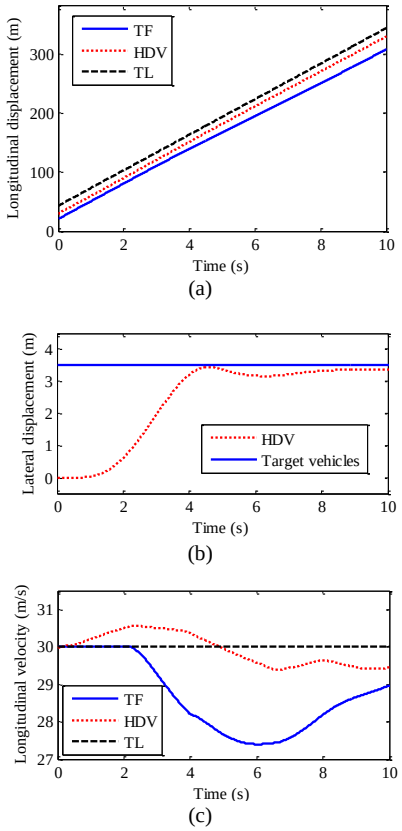

Figs. 15. Profiles of (a) longitudinal displacement, (b) lateral displacement, and (c) longitudinal velocity of the HDV and target vehicles in the discretionary cut-in (beyond the preventable range) test.

Figs. 15 (a), (b), and (c) show the profiles of the longitudinal displacement, lateral displacement, and longitudinal velocity of the vehicles in the discretionary cut-in (beyond the preventable range) test, respectively. We see the HDV speeds up and makes lateral movement to perform the cut-in towards the VP in the beginning. Then, it completes the cut-in maneuver and adjusts its velocity to follow the TL. The TF keeps a constant distance from the TL in the beginning, then slows down to yield to the HDV, and finally adjusts the velocity to follow the HDV.

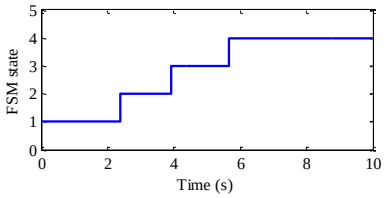

Fig. 16. FSM state of the proposed method in the discretionary cut-in (from within to beyond the preventable range) test.

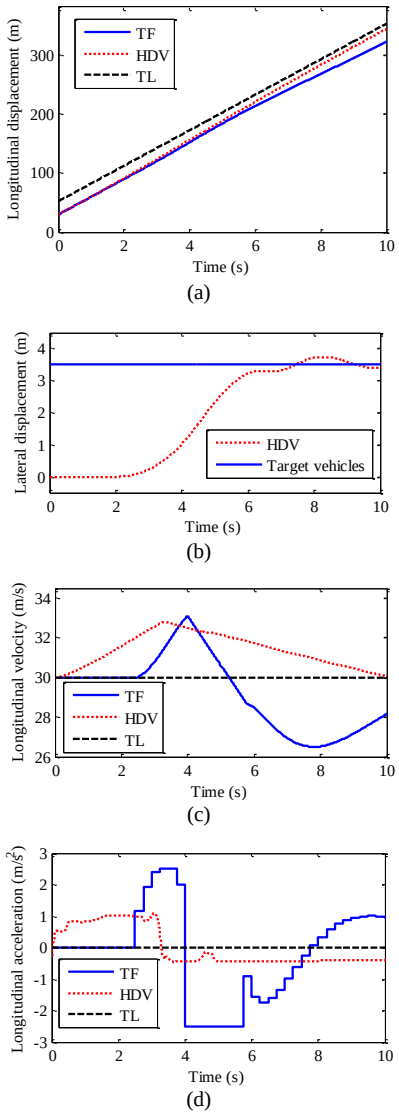

Figs. 17. Profiles of (a) longitudinal displacement, (b) lateral displacement, (c) longitudinal velocity, and (d) longitudinal acceleration of the HDV and target vehicles in the discretionary cut-in (from within to beyond the preventable range) test.

3) Cut-in from within to beyond Preventable Range

Fig. 16 shows the FSM state of the proposed method in addressing the discretionary cut-in from within to beyond the preventable range. We see the FSM state is switched from the CF state (following the TL) to the cut-in prevention state at 2.4 s, when the HDV is detected to have a cut-in intention and within the preventable range. Then, the FSM state is switched to the cut-in yielding state at 3.9 s when the HDV is beyond the preventable range. Finally, the FSM state is switched to the CF state (following the cut-in vehicle) at 5.7 s, when the HDV reaches the target lane.

Figs. 17 (a), (b), (c), and (d) show the profiles of the longitudinal displacement, lateral displacement, longitudinal velocity, and longitudinal acceleration of the vehicles in the discretionary cut-in (from within to beyond the preventable range) test, respectively. We see that the HDV speeds up to overtake the TF in the beginning. Then, even though the TF speeds up to shorten the platoon gap, the HDV continues to speed up and makes lateral movement. After that, it completes the cut-in maneuver and slows down to follow the TL. The TF maintains a constant distance from the TL in the beginning. Then, it accelerates to shorten the platoon gap. Next, it decelerates to yield to the HDV. Finally, it adjusts the velocity to follow the HDV. According to the acceleration profile, the acceleration constraints are not violated in the whole driving process. Note that, since simple kinematic models are used to simulate the target vehicles in the simulation environment, the speed of the TF can be indifferentiable at certain points, especially at the state transition points.

VII. Discussion and Conclusion

To address the cut-in maneuver of the HDVs, this paper has proposed an intention prediction-based control method for the VPs by considering the tradeoff between the platoon integrity and traffic safety. Particularly, the proposed method is built to prevent as many cut-ins as possible while taking care of the road safety. It includes a cut-in prediction part, consisting of a cut-in intention prediction algorithm and a vehicle trajectory prediction algorithm, and an FSM-based predictive control part, which include a high-level FSM and a low-level predictive control. Driver-in-the-loop experiments were conducted in the VP-based driving scenarios to train the intention prediction algorithm and test the proposed method. According to five times five-fold cross validation, the algorithm achieves an average accuracy of 93.1% as the time window length of the driving data increases to 4 s. We show the results of a no cut-in test, a mandatory cut-in test, and three discretionary cut-in tests. In the results, we analyze the control process of the proposed method according to its FSM state and the states of the HDV and target vehicles. The results show that the proposed method can predict the cut-in intention of human drivers in real time. Besides, it can prevent cut-ins for the VP while taking care of the road safety according to the results of the prediction algorithms.

Several issues about the proposed method should be noted. Firstly, it focuses on the decision making and vehicle control parts of the autonomous driving process. Perception delays,

errors, and failures, which are typically handled in vehicle perception part, are out of scope for this study. In practice, a combination of multiple sensors, such as inertial measurement units, odometers, and cameras, can be used to improve the perception accuracy, reliability, and robustness [29]. In the case of faulty perception, fault detection and isolation systems should be first used to detect and identify perception failures and then safety measures, such as pull over, should be conducted to ensure the road safety [29].

Secondly, the proposed method was tested under simulation environment, where ideal perception was assumed. However, in real scenarios, perception delays and errors of surroundings and vehicle states may exist, even when advanced sensing techniques and computer vision algorithms are deployed [41]. Before applying the proposed method in real scenarios, we should test it with a real vehicle in real environments.

Thirdly, the intention prediction algorithm may fail to predict the intention of human drivers. The following two cases can happen. First, an HDV without cut-in intention is detected as a cut-in vehicle; the FSM enters the cut-in prevention or yielding states to respond to the false alarm. This case can result in the unnecessary response of the VP. A possible remediation of this case is to make adaptive adjustment of the VP according to the subsequence states of the predicted vehicle. Our future work will focus on this direction. Second, a cut-in vehicle is detected as an HDV without cut-in intention; the FSM remains in the CF state until the cut-in vehicle is predicted to drive across the lane mark. This case is potentially dangerous. We apply the vehicle trajectory prediction algorithm to address this issue. Once the vehicle is predicted to drive across the lane mark by the trajectory prediction algorithm, the FSM is switched from the CF state to the cut-in yielding state for the road safety.

Fourthly, the proposed method controls the VP based on the prediction of the driver intention and vehicle trajectory. The prediction can help the VPs better assess the potential cut-ins and respond to the cut-ins as early as possible. Particularly, the FSM-based control part switches control strategies based on the results of the prediction algorithms. The intention prediction algorithm performs well with the average accuracy up to 93.1%. Since a higher prediction accuracy of the intention prediction algorithm can enable the FSM-based control part to perform more accurate control and work more efficiently, our future work should further improve the prediction accuracy of the driver intention.

ACKNOWLEDGMENT

The authors would like to thank the volunteers for their participation in the experiments.

REFERENCES

[1] R. Hall and C. Chin, "Vehicle sorting for platoon formation: Impacts on highway entry and throughput," *Transportation Research Part C: Emerging Technologies*, vol. 13, no. 5–6, pp. 405–420, Dec. 2005.

[2] J. Lioris, R. Pedarsani, F. Y. Tascikaraoglu, and P. Varaiya, "Platoons of connected vehicles can double throughput in urban roads," *Transportation Research Part C: Emerging Technologies*, vol. 77, pp. 292–305, Apr. 2017.

[3] L. Xu, L. Wang, G. Yin, and H. Zhang, "Communication information structures and contents for enhanced safety of highway vehicle platoons," *IEEE Transactions on Vehicular Technology*, vol. 63, no. 9, pp. 4206–4220, Nov. 2014.

[4] K. C. Dey, L. Yan, X. Wang, Y. Wang, H. Shen, M. Chowdhury, L. Yu, C. Qiu, and V. Soundararaj, "A review of communication, driver characteristics, and controls aspects of cooperative adaptive cruise control (CACC)," *IEEE Transactions on Intelligent Transportation Systems*, vol. 17, no. 2, pp. 491–509, Feb. 2016.

[5] K. Liang, J. Mårtensson, and K. H. Johansson, "Heavy-duty vehicle platoon formation for fuel efficiency," *IEEE Transactions on Intelligent Transportation Systems*, vol. 17, no. 4, pp. 1051–1061, Apr. 2016.

[6] B. Wang, and R. Su, "A distributed platoon control framework for connected automated vehicles in an urban traffic network," *IEEE Transactions on Control of Network Systems*, online.

[7] H. Farah, S. M. Erkens, T. Alkim, and B. van Arem, "Infrastructure for automated and connected driving: State of the art and future research directions," *Road vehicle automation 4*, pp. 187–197, 2018.

[8] T. Zhang, D. Tao, X. Qu, X. Zhang, R. Lin, and W. Zhang, "The roles of initial trust and perceived risk in public's acceptance of automated vehicles," *Transportation research part C: emerging technologies*, vol. 98, pp. 207–220, Jan. 2019.

[9] S. E. Shladover, "Connected and automated vehicle systems: Introduction and overview," *Journal of Intelligent Transportation Systems*, vol. 22, pp. 190–200, May 2018.

[10] M. Aramrattana, T. Larsson, C. Englund, J. Jansson, and A. Nåbo, "A simulation study on effects of platooning gaps on drivers of conventional vehicles in highway merging situations," *IEEE Transactions on Intelligent Transportation Systems*, vol. 23, no. 4, pp. 3790–3796, Dec. 2020.

[11] J. Axelsson, "Safety in vehicle platooning: A systematic literature review," *IEEE Transactions on Intelligent Transportation Systems*, vol. 18, no. 5, pp. 1033–1045, May. 2017.

[12] X. Wang, M. Yang, and D. Hurwitz, "Analysis of cut-in behavior based on naturalistic driving data," *Accident Analysis & Prevention*, vol. 124, pp. 127–137, Mar. 2019.

[13] Y. Chen, C. Hu, and J. Wang, "Human-centered trajectory tracking control for autonomous vehicles with driver cut-in behavior prediction," *IEEE Transactions on Vehicular Technology*, vol. 68, no. 9, pp. 8461–8471, Sep. 2019.

[14] R. Fu, Z. Li, Q. Sun, and C. Wang, "Human-like car-following model for autonomous vehicles considering the cut-in behavior of other vehicles in mixed traffic," *Accident Analysis & Prevention*, vol. 132, pp.105260, Nov. 2019.

[15] Q. Chen, W. Zhao, L. Li, C. Wang, and F. Chen, "ES-DQN: A learning method for vehicle intelligent speed control strategy under uncertain cut-in scenario," *IEEE Transactions on Vehicular Technology*, vol. 71, no. 3, pp. 2472–2484, Mar. 2022.

[16] Y. Zhang, Q. Lin, J. Wang, S. Verwer, and J. M. Dolan, "Lane-change intention estimation for car-following control in autonomous driving," *IEEE Transactions on Intelligent Vehicles*, vol. 3, no. 3, pp. 276–286, Sep. 2018.

[17] K. Choi, H. G. Jung, "Cut-in vehicle warning system exploiting multiple rotational images of SVM camera", *Expert Systems with Application*, vol. 125, pp. 81-99, Jul. 2019.

[18] N. Lyu, J. Wen, Z. Duan, and C. Wu, "Vehicle trajectory prediction and cut-in collision warning model in a connected vehicle environment," *IEEE Transactions on Intelligent Transportation Systems*, vol. 23, no. 2, pp. 966–981, Feb. 2022.

[19] V. Milanés and S. E. Shladover, "Handling cut-in vehicles in strings of cooperative adaptive cruise control vehicles," *Journal of Intelligent Transportation Systems*, vol. 20, no. 2, pp. 178–191, 2016.

[20] S. Bang and S. Ahn, "Control of connected and autonomous vehicles with cut-in movement using spring mass damper system," *Transportation Research Record*, vol. 2672, no. 20, pp. 133–143, Dec. 2018.

[21] H. Kazemi, H. N. Mahjoub, A. Tahmasbi-Sarvestani, and Y. P. Fallah, "A learning-based stochastic MPC design for cooperative adaptive cruise control to handle interfering vehicles," *IEEE Transactions on Intelligent Vehicles*, vol. 3, no. 3, pp. 266–275, Sep. 2018.

[22] M. H. Basiri, B. Ghojogh, N. L. Azad, S. Fischmeister, F. Karray, and M. Crowley, "Distributed nonlinear model predictive control and metric learning for heterogeneous vehicle platooning with cut-in/cut-out maneuvers," *in 2020 59th IEEE Conference on Decision and Control (CDC)*. IEEE, pp. 2849–2856, 2020.

[23] H. Yao and X. Li, "Lane-change-aware connected automated vehicle trajectory optimization at a signalized intersection with multi-lane roads,"

Transportation Research Part C: Emerging Technologies, vol. 129, p.103182, Aug. 2021.
[24] M. Liu, S. Rathinam, M. Lukuc, and S. Gopalswamy, "Fusing radar and vision data for cut-in vehicle identification in platooning applications," *SAE International Journal of Advances and Current Practices in Mobility*, vol. 2, no. 6, pp.3044–3050, 2020.
[25] P. Kumar, M. Perrollaz, S. Lefevre, and C. Laugier, "Learning-based approach for online lane change intention prediction," In *2013 IEEE Intelligent Vehicles Symposium (IV)*, pp. 797–802, Jun. 2013.
[26] Y. Lu, and L. Bi, "Human behavior model-based predictive control of longitudinal brain-controlled driving," *IEEE Transactions on Intelligent Transportation Systems*, vol. 22, no. 3, pp. 1361–1374, Mar. 2021.
[27] A. Gray, M. Ali, Y. Gao, J. K. Hedrick, and F. Borrelli, "A unified approach to threat assessment and control for automotive active safety," *IEEE Transactions on Intelligent Transportation Systems*, vol. 14, no. 3, pp. 1490–1499, Sep. 2013.
[28] Y. Lu, L. Bi, and H. Li, "Model predictive-based shared control for brain-controlled driving," *IEEE Transactions on Intelligent Transportation Systems*, vol. 21, no. 2, pp. 630–640, Feb. 2020.
[29] J. Van Brummelen, M. O'Brien, D. Gruyer, and H. Najjaran, "Autonomous vehicle perception: The technology of today and tomorrow," *Transportation research part C: emerging technologies*, vol. 89, pp. 384–406, Apr. 2018.
[30] C. C. Chang and C. J. Lin. *LIBSVM—A Library for Support Vector Machines*. Accessed: 2001. [Online]. Available: http://www.csie.ntu.edu.tw/~cjlin/libsvm/
[31] J. P. Marques de Sá, *Pattern Recognition: Concepts, Methods and Applications*. Berlin, Germany: Springer-Verlag, 2012.
[32] S. Amari and S. Wu, "Improving support vector machine classifiers by modifying kernel functions," *Neural Netw.*, vol. 12, no. 6, pp. 783–789, Jul. 1999.
[33] Y. Lu, B. Wang, L. Huang, N. Zhao, and R. Su, "Modeling of driver cut-in behavior towards a platoon," *IEEE Transactions on Intelligent Transportation Systems*, early access, Sep. 2022.
[34] R. Dang, J. Wang, S. E. Li, and K. Li, "Coordinated adaptive cruise control system with lane-change assistance," *IEEE Transactions on Intelligent Transportation Systems*, vol. 16, no. 5, pp. 2373–2383, Oct. 2015.
[35] Y. Ali, Z. Zheng, and M. M. Haque, "Modelling lane-changing execution behaviour in a connected environment: A grouped random parameters with heterogeneity-in-means approach," *Communications in Transportation Research*, vol. 1, Dec. 2021, Art. no. 100009.
[36] V. Bageshwar, W. Garrard, and R. Rajamani, "Model predictive control of transitional maneuvers for adaptive cruise control vehicles," *IEEE Transactions on Vehicular Technology*, vol. 53, no. 5, pp. 1573–1585, Sep. 2004.
[37] D. Swaroop, J. K. Hedrick, C. C. Chien, and P. Ioannou, "A comparision of spacing and headway control laws for automatically controlled vehicles," *Vehicle System Dynamics*, vol. 23, no. 1, pp. 597–625, 1994.
[38] A. Ali, G. Garcia, and P. Martinet, "The flatbed platoon towing model for safe and dense platooning on highways," *IEEE Intelligent Transportation Systems Magazine*, vol. 7, no. 1, pp. 58–68, Jan. 2015.
[39] Y. Zheng, S. E. Li, J. Wang, D. Cao, and K. Li, "Stability and scalability of homogeneous vehicular platoon: Study on the influence of information flow topologies," *IEEE Transactions on Intelligent Transportation Systems*, vol. 17, no. 1, pp. 14–26, Jan. 2016.
[40] S. Boyd and L. Vandenberghe, *Convex Optimization*. Cambridge, U.K.: Cambridge Univ. Press, 2004.
[41] A. B. Hillel, R. Lerner, D. Levi, and G. Raz, "Recent progress in road and lane detection: A survey," *Machine Vision and Applications*, vol. 25, no. 3, pp. 727–745, Apr. 2014

Yun Lu (S'19-M'20) received the Ph. D. degree in mechanical engineering from Beijing Institute of Technology, Beijing, China, in 2020.

He is currently a Research Fellow with the School of Electrical and Electronic Engineering, Nanyang Technological University, Singapore. From Jan. 2019 to Mar. 2020, he was a visiting scholar with the Department of Mechanical Engineering, University of Michigan, Ann Arbor, MI, USA. His research interests include human behavior modeling, platoon control, driver assistance system, machine learning, and brain-control driving. He is an author of several refereed journal articles in the IEEE TRANSACTIONS ON INTELLIGENT TRANSPORTATION SYSTEMS and IEEE TRANSACTIONS ON NEURAL SYSTEMS AND REHABILITATION ENGINEERING. He was selected as an outstanding graduate in Beijing in 2020.

Lingying Huang received her B.S. degree in Electrical Engineering and Automation from Southeast University, JiangSu, China, in 2017, and the Ph.D degree in Electrical and Computer Engineering from Hong Kong University of Science and Technology, Hong Kong, in 2021.

She is currently a Research fellow at the School of Electrical and Electronic Engineering, Nanyang Technological University. From July 2015 to August 2015, she had a summer program in Georgia Tech Univerisity, USA. Her current research interests include intelligent vehicles, cyber-physical system security/privacy, networked state estimation, event-triggered mechanism and distributed optimization.

Jiarong Yao received the B.S. degree in traffic engineering in 2016 and the Ph.D. degree in department of comprehensive traffic information and control engineering in 2021, both from Tongji University. Now she is a research fellow in School of Electrical and Electronic Engineering, Nanyang Technological University. Her main research interest is traffic control and Intelligent Transportation Systems.

Rong Su (M’11–SM’14) obtained his Bachelor of Engineering degree from University of Science and Technology of China, and Master of Applied Science degree and PhD degree from University of Toronto, respectively. He was affiliated with University of Waterloo and Technical University of Eindhoven before he joined Nanyang Technological University in 2010. Dr Su's research interests include multi-agent systems, discrete-event system theory, model-based fault diagnosis, cyber security analysis and synthesis, control and optimization of complex networks with applications in flexible manufacturing, intelligent transportation, human-robot interface, power management and green buildings. In the aforementioned areas he has more than 270 journal and conference publications, 1 monograph, 16 granted/filed patents.

Dr Su is a senior member of IEEE, and an associate editor for Automatica (IFAC), Journal of Discrete Event Dynamic Systems, and Journal of Control and Decision. He was the Chair of the Technical Committee on Smart Cities in the IEEE Control Systems Society in 2016-2019. Currently, he is a co-chair of Technical Committee on Automation in Logistics in the IEEE Robotics and Automation Society. Dr Su is a co-author of several best conference/journal paper awards, e.g., 2021 Hsue-shen Tsien Paper Award from IEEE/CAA Journal of Automatica Sinica and the Best Paper Award in the 15th International Conference on Advanced Systems in Public Transport (CASPT2022). He is a Distinguished Lecturer for 2020 Chinese Conference on Decision and Control (CCDC'20) and an IEEE Distinguished Lecturer for IEEE Robotics and Automation Society.